

A non-intrusive approach for proper orthogonal decomposition modal coefficients reconstruction through active subspaces

Nicola Demo^{*}, Marco Tezzele[†] and Gianluigi Rozza[‡]

Mathematics Area, mathLab, SISSA, International School of Advanced Studies, via Bonomea 265, I-34136 Trieste, Italy

May 8, 2022

Abstract

Reduced order modeling (ROM) provides an efficient framework to compute solutions of parametric problems. Basically, it exploits a set of precomputed high-fidelity solutions — computed for properly chosen parameters, using a full-order model — in order to find the low dimensional space that contains the solution manifold. Using this space, an approximation of the numerical solution for new parameters can be computed in real-time response scenario, thanks to the reduced dimensionality of the problem. In a ROM framework, the most expensive part from the computational viewpoint is the calculation of the numerical solutions using the full-order model. Of course, the number of collected solutions is strictly related to the accuracy of the reduced order model. In this work, we aim at increasing the precision of the model also for few input solutions by coupling the proper orthogonal decomposition with interpolation (PODI) — a data-driven reduced order method — with the active subspace (AS) property, an emerging tool for reduction in parameter space. The enhanced ROM results in a reduced number of input solutions to reach the desired accuracy. In this contribution, we present the numerical results obtained by applying this method to a structural problem and in a fluid dynamics one.

1 Introduction

In a large variety of engineering and computational science fields, reduced order modeling (ROM) has gained more and more popularity to treat para-

^{*}nicola.demo@sissa.it

[†]marco.tezzele@sissa.it

[‡]gianluigi.rozza@sissa.it

metric problems thanks to its capability to drastically reduce the computational cost required for the numerical solutions [30, 29]. Despite the progresses in the global amount of computational power, many problems still remain intractable using only the conventional discretization methods — e.g. finite element, finite volume — especially in a many-queries or real-time context. The idea behind ROM is that a generic problem, even very complex, has an intrinsic dimension much lower than the number of degrees of freedom of the discretized system. To achieve this dimensionality reduction, a database of several solution is firstly collected by solving the original high-order model for different parameters (physical or geometrical). Then, all the solutions are combined to build the space onto which we can accurately project the solution manifold and efficiently compute the solutions for the new parameters. We typically call *offline phase* the initial step in which many high-fidelity solutions are computed and, depending from the studied problem, it can be very demanding from the computational viewpoint. The second step, the *online phase*, is instead very fast since only the solution of the low-dimensional problem has to be performed.

The accuracy of the reduced order model depends by the problem itself, by the number of parameters and the number of snapshots collected during the offline phase. In this work, we use a non-intrusive proper orthogonal decomposition with interpolation (PODI) method [6] for the data-driven dimensionality reduction, coupling it to the active subspace (AS) property [7].

PODI is an equation-free method based on proper orthogonal decomposition capable to build a reduced order model without any knowledge about the equations of the original problem, requiring just the $(\boldsymbol{\mu}, \mathbf{u})$ pairs, where $\boldsymbol{\mu}$ refers to the input parameters and \mathbf{u} to the corresponding parametric solution. Further insights and industrial applications of data-driven ROMs can be found in [38]. Instead, AS is an emerging tool for the reduction of the parameter space dimensionality. Basically, it aims to approximate a scalar function with multi-dimensional input with a new function whose input parameters are linear combinations of the original parameters. This parameter space reduction enhances the accuracy of the reduced order model, thanks to the simplification of the parametric formulation, overcoming the curse of dimensionality. For a more exhaustive introduction on ROMs and parameters space reduction, we recommend [27], while for the improvement of reduced order models thanks to AS property, we mention [39] for some preliminary results in naval application using data-driven approach, and [36] as an example of enhanced POD-Galerkin method applied to a biomedical problem.

In this work we are going to present an original application of the active subspace property for the reconstruction of the modal coefficients of the proper orthogonal decomposition. Moreover we demonstrate that this results in better interpolation capabilities for the PODI when we have a small amount of snapshots collected in the offline phase. This coupling is

especially useful when we have a very limited computational budget.

The work is organised as follows: in Section 2 we present the POD and the POD with interpolation as a data-driven approach for ROMs; in Section 3 we briefly introduce the active subspaces property; in Section 4 we show the application of the proposed method on two simple parametric problems: a structural analysis problem and a computational fluid dynamics problem. Finally some perspective and future developments are presented.

2 Reduced order modeling through proper orthogonal decomposition with interpolation

Proper orthogonal decomposition (POD) is a widespread technique in the reduced order modeling (ROM) community for the study of parametric problems, thanks to its capacity to extract, from a set of high-dimensional snapshots, the basis minimizing the error between the original snapshots and their orthogonal projection. Let \mathbb{V}^N be the high-dimensional discrete space which the snapshots belong to. The basis $\{\phi_1, \phi_2, \dots, \phi_{Ns}\} \in \mathbb{V}^N$ spans the POD space $\mathbb{V}^{Ns} \subset \mathbb{V}^N$ which, by construction, is the optimal space of dimension Ns to represent the snapshots, where ϕ_i for $i = 1, 2, \dots, Ns$ are the so-called POD modes.

We can project the equations of the full-order problem onto the POD space in order to obtain a low-dimensional representation of the original operators. Since the number of degrees of freedom N of the initial problem is usually much greater than the reduced dimension Ns , the numerical solution of the reduced order model results inexpensive from the computational viewpoint. This method is called POD-Galerkin: for further details about this approach we suggest, among many different works, for example [18, 3, 35, 21, 34, 10, 19].

The data-driven approach — also named non-intrusive — used in this work does not require the original equations. The original snapshots are projected onto the POD space in order to reduce their dimensionality then the solution manifold is approximated using an interpolation technique. Examples of application of this so-called POD with interpolation (PODI) [5, 6] method can be found in literature: for naval engineering problem we cite [12, 11, 13], for automotive [31, 15] and for aeronautics [26]. A coupling with isogeometric analysis can be found in [17].

Let now focus on the computation of the POD modes. Let \mathbf{u}_i , with $i = 1, \dots, Ns$, be the snapshots collected by solving the high-dimensional problem, with different values of the input parameters $\boldsymbol{\mu}_i$, resulting in Ns input-output pairs $(\boldsymbol{\mu}_i, \mathbf{u}_i)$. The snapshots matrix \mathbf{S} is constructed arranging the snapshots as columns, such that $\mathbf{S} = [\mathbf{u}_1 \ \mathbf{u}_2 \ \dots \ \mathbf{u}_{Ns}]$. We apply the singular value decomposition to this matrix to obtain:

$$\mathbf{S} = \mathbf{U}\mathbf{\Sigma}\mathbf{V}^* \approx \mathbf{U}_k\mathbf{\Sigma}_k\mathbf{V}_k^*, \quad (1)$$

where $\mathbf{U} \in \mathbb{A}^{N \times Ns}$ is the unitary matrix containing the left-singular vectors, $\mathbf{\Sigma} \in \mathbb{A}^{Ns \times Ns}$ is the diagonal matrix containing the singular values λ_i , and $\mathbf{V} \in \mathbb{A}^{Ns \times Ns}$, with the symbol $*$ denoting the conjugate transpose. The left-singular vectors, namely the columns of \mathbf{U} , are the so-called POD modes. It is important to note that the magnitude of the singular values describes the energy of the corresponding modes. We can keep the first k modes to span the optimal space with dimension k to represent the snapshots. Since the singular values are returned in decreasing order, we can truncate the number of modes simply selecting the first k columns of \mathbf{U} . The matrices $\mathbf{U}_k \in \mathbb{A}^{N \times k}$, $\mathbf{\Sigma}_k \in \mathbb{A}^{k \times k}$, $\mathbf{V}_k \in \mathbb{A}^{Ns \times k}$ in Equation (1) are the truncated matrices with rank k . We can also measure the error, in Euclidean and Frobenius norm, introduced by the truncation [25]:

$$\|\mathbf{S} - \mathbf{U}_k \mathbf{\Sigma}_k \mathbf{V}_k^*\|_2^2 = \lambda_{k+1}^2, \quad (2)$$

$$\|\mathbf{S} - \mathbf{U}_k \mathbf{\Sigma}_k \mathbf{V}_k^*\|_F = \sqrt{\sum_{i=k+1}^{Ns} \lambda_i^2}. \quad (3)$$

After constructing the POD space, we can project the original snapshots onto this space. In matrix form, we compute $\mathbf{C} \in \mathbb{R}^{k \times Ns}$ as $\mathbf{C} = \mathbf{U}_k^T \mathbf{S}$, where the columns of \mathbf{C} are the low-dimensional representation of the input, the so-called modal coefficients. Practically, we can express the input snapshots as a linear combination of the modes using these coefficients. Formally:

$$\mathbf{u}_i = \sum_{j=1}^{Ns} \alpha_{ji} \phi_j \approx \sum_{j=1}^k \alpha_{ji} \phi_j, \quad \forall i \in [1, 2, \dots, Ns], \quad (4)$$

where α_{ji} are the elements of \mathbf{C} . Finally, we obtain the $(\boldsymbol{\mu}_i, \alpha_i)$ pairs, for $i = 1, 2, \dots, Ns$, that sample the solution manifold in the parametric space. We are able to interpolate the modal coefficients α and for any new parameter approximate the new coefficients. At the end, we compute the high-dimensional solution by projecting back the (approximated) modal coefficients to the original space by using Equation (4).

Regarding the technical implementation of the PODI method, we adopt the Python package called EZyRB [14].

3 Active subspaces for modal coefficient reconstruction

Active subspaces property [7, 8] is a powerful technique developed for parameter studies. The idea is to perform a sensitivity analysis of the function of interest with respect to the parameters, while reducing the parameter space dimensionality.

We want to unveil specific directions in the parameter space along which the scalar function of interest varies the most on average. This is done by rescaling the inputs in a reference domain centered in the origin and then by rotating the parameter space until a lower dimensional structure is highlighted. A drawback of this technique is that every function with a radial symmetry does not have an active subspace since there are no preferred directions to rotate the domain. Nevertheless a wide range of functions of interest in engineering applications present an active subspace of dimension one or two, resulting in a great reduction of the parameter space. Among others we cite shape optimization [22], and uncertainty quantification in the numerical simulation of the HyShot II screamjet [9]. We would also like to mention some naval engineering applications of the active subspaces: coupled with boundary element method and free form deformation [40], for propeller blade design [23], and a shared subspace application for constraint optimisation [37].

Let f be a parametric scalar function of interest $f(\boldsymbol{\mu}) : \mathbb{R}^p \rightarrow \mathbb{R}$, and $\rho : \mathbb{R}^p \rightarrow \mathbb{R}^+$ a probability density function representing uncertainty in the input parameters $\boldsymbol{\mu} \in \mathbb{R}^p$. Active subspaces are a property of the pair (f, ρ) . To discover if a pair has an active subspace of dimension M , we need to construct the uncentered covariance matrix $\boldsymbol{\Sigma}$ of the gradients of f with respect to the input parameters, $\nabla f(\boldsymbol{\mu}) \in \mathbb{R}^p$, that reads:

$$\boldsymbol{\Sigma} = \mathbb{E} [\nabla_{\boldsymbol{\mu}} f \nabla_{\boldsymbol{\mu}} f^T] = \int (\nabla_{\boldsymbol{\mu}} f)(\nabla_{\boldsymbol{\mu}} f)^T \rho d\boldsymbol{\mu}, \quad (5)$$

where \mathbb{E} is the expected value, and $\nabla_{\boldsymbol{\mu}} f \equiv \nabla f(\boldsymbol{\mu})$. Since $\boldsymbol{\Sigma}$ is symmetric it has a real eigenvalue decomposition:

$$\boldsymbol{\Sigma} = \mathbf{W} \boldsymbol{\Lambda} \mathbf{W}^T, \quad (6)$$

where \mathbf{W} is an orthogonal matrix containing the eigenvectors of $\boldsymbol{\Sigma}$ as columns, and $\boldsymbol{\Lambda}$ is a diagonal matrix composed by the non-negative eigenvalues arranged in descending order.

We are looking at spectral gap in order to identify the proper dimension $M < p$ of the active subspace. In particular, we define the active subspace of dimension M as the span of the first M eigenvectors of \mathbf{W} , which correspond to the first eigenvalues before a significant spectral gap. We proceed by decomposing the two matrices as follows

$$\boldsymbol{\Lambda} = \begin{bmatrix} \boldsymbol{\Lambda}_1 & \\ & \boldsymbol{\Lambda}_2 \end{bmatrix}, \quad \mathbf{W} = [\mathbf{W}_1 \quad \mathbf{W}_2], \quad \mathbf{W}_1 \in \mathbb{R}^{p \times M}. \quad (7)$$

Then we can map the full parameters to the reduced ones through \mathbf{W}_1 . We define the active variable as $\boldsymbol{\mu}_M = \mathbf{W}_1^T \boldsymbol{\mu} \in \mathbb{R}^M$, and the inactive variable as $\boldsymbol{\eta} = \mathbf{W}_2^T \boldsymbol{\mu} \in \mathbb{R}^{p-M}$. The eigenvectors represent the weights of the linear combination of the input parameters, thus providing a sensitivity of each

parameter. If a weight is almost zero, that means f does not vary along that direction on average.

With the active variable we can build a surrogate model g to approximate the function of interest, that is

$$f(\boldsymbol{\mu}) \approx g(\mathbf{W}_1^T \boldsymbol{\mu}) = g(\boldsymbol{\mu}_M). \quad (8)$$

The error upper bound for the approximation of f through a response surface depends on the square root of the sum of the eigenvalues corresponding to the active variables times the eigenvectors approximation error ϵ , plus the square root of the sum of the remaining eigenvalues [7]:

$$\text{RMSE} \leq C_1 \left[\epsilon \left(\sum_{i=1}^M \lambda_i \right)^{1/2} + \left(\sum_{i=M+1}^p \lambda_i \right)^{1/2} \right] + C_2, \quad (9)$$

with C_1 and C_2 prescribed constants.

4 Numerical results

In this section we are going to present two different test cases: the first in the context of linear structural analysis, and the second in computational fluid dynamics.

We sample the parameter space \mathbb{P} with a uniform density function, obtaining 200 samples for both the problems. The actual space \mathbb{P} will be defined in the corresponding sections. To split the dataset for training and test purpose we use a k -fold cross-validation (CV) [20], with $k = 5$. First we randomly partition the samples into k equal sized subsamples. Among these k sets, a single one is retained to validate the model, and the remaining $k - 1$ are used as training data. We repeat the cross-validation process k times, with each of the k subsamples used exactly once as test data. Then the results are then averaged to produce a single estimation. One of the advantages of this method over repeated random sub-sampling is that all samples are used for both training and testing, and each observation is used for validation exactly once.

We are interested in the relative reconstruction error of the two output fields of interest: the stress tensor in the first example, and the pressure field in the second one. The error is computed as the average over the test samples of the norm of the difference between the exact and the approximated solution over the norm of the exact solution.

We approximate the stress tensor field and the pressure field by using ridge functions [24] g_i to reconstruct the modal coefficients through active subspaces. The modal coefficients corresponding to the parameter sample $\boldsymbol{\mu}^*$ are $\alpha(\boldsymbol{\mu}^*) \equiv \alpha^* = [\alpha_1^*, \dots, \alpha_N^*]^T$. The actual approximation of the modal

coefficient is defined as follows

$$\alpha_i^* \approx g_i(\mathbf{W}_{1,i}^T \boldsymbol{\mu}^*) \quad i \in [1, \dots, N], \quad (10)$$

where $\mathbf{W}_{1,i}$ is the first eigenvector defining the active subspace of dimension one corresponding to the i -th modal coefficient, and g_i a response function. We select only the first eigenvector because every single modal coefficient presents an active subspace of dimension one as shown in the following sections.

Recalling Equation (4), we have the new approximated representation of the snapshots \mathbf{u}_i , using the corresponding k response functions g_{ji} :

$$\mathbf{u}_i = \sum_{j=1}^{Ns} \alpha_{ji} \phi_j \approx \sum_{j=1}^k \alpha_{ji} \phi_j \approx \sum_{j=1}^k g_{ji}(\mathbf{W}_{1,j}^T \boldsymbol{\mu}) \phi_j, \quad \forall i \in [1, 2, \dots, Ns]. \quad (11)$$

4.1 Numerical study 1: stress tensor field reconstruction of a parametrised beam

We consider a double-T beam with both ends fixed, and we apply a uniform load condition. The length of the beam is 9000 mm, the height of the beam is 450 mm, the span of the upper flange is equal to 500 mm, and the span of the lower flange is 100 mm. The uniform load is 8.7 KN/m. The input parameters $\boldsymbol{\mu} \in \mathbb{R}^p$ represent the thickness of specific regions of the beam. We divided the beam in three equidistant sections along the longitudinal direction, and we preserve the symmetry by imposing the same thickness on the external sections. The actual parameters are $\boldsymbol{\mu} \in \mathbb{P} := [5.0, 10.0]^6$, and the sampling is done using a uniform probability density function. They are defined as in Table 1. The equations governing the linear elastic isotropic problem are the equilibrium equation, the linearised small-displacement strain-displacement relationship, and the Hooke's law, respectively:

$$\begin{cases} -\nabla \cdot \boldsymbol{\sigma} = f, \\ \boldsymbol{\epsilon} = \frac{1}{2}[\nabla u + \nabla u^T], \\ \boldsymbol{\sigma} = C(E, \nu) : \boldsymbol{\epsilon}, \end{cases} \quad (12)$$

where $\boldsymbol{\sigma}$ is the Cauchy stress tensor, f is the body force, $\boldsymbol{\epsilon}$ is the infinitesimal strain tensor, u is the displacement vector, and C is the fourth-order stiffness tensor depending on E , the Young modulus, and on ν , the Poisson's ratio. In Figure 1 an example of a possible deformation of the beam from two different views.

Table 1: Description of the input parameters μ_i , representing the thickness of particular sections of the beam. Lower and upper bounds are highlighted in mm.

Parameter	Section of the beam	Lower bound	Upper bound
μ_1	External sections web	5.0	10.0
μ_2	Internal section web	5.0	10.0
μ_3	External sections lower flange	5.0	10.0
μ_4	Internal section lower flange	5.0	10.0
μ_5	External sections upper flange	5.0	10.0
μ_6	Internal section upper flange	5.0	10.0

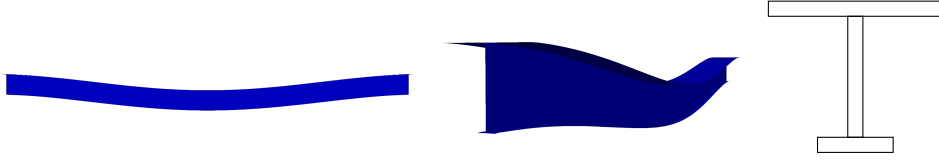


Figure 1: Two different views of a deformed beam after the application of a magnification factor equal to 100 along the z-direction. On the right the longitudinal section of the beam.

We compute the POD modes and coefficients as explained in Section 2. In particular we truncate the modal expansion to the first 6 modes. This choice is made in accordance to the singular values decay as depicted in Figure 2 on the left. After the computation of the modal coefficients we approximate the active subspace of dimension 1 for each coefficient. Following Equation (10) we are able to approximate the coefficients using a univariate function. As response surface g we use gaussian process regression with a radial basis function kernel. The comparison with the interpolation of the single coefficients using the full parameter space is presented in Figure 2 on the right. For the *standard* procedure we mean the use of radial basis functions interpolation in order to approximate the functions $\mu \in \mathbb{P} \rightarrow \alpha_i(\mu)$, with $i \in [1, \dots, 6]$. The relative error is computed as describe above using a 5-fold cross validation method, and is expressed as a function of the cardinality of the samples set (both for training and testing). We can see that active subspaces allow smaller reconstruction error for a given number of samples up to a certain threshold, 44 training samples in this case. This means that, for a given small computational budget devoted to the offline phase, we can gain around 1% in terms of relative error. The reconstruction error in the AS case does not improve increasing the samples because we have already reached intrinsic error of the active subspaces approximation.

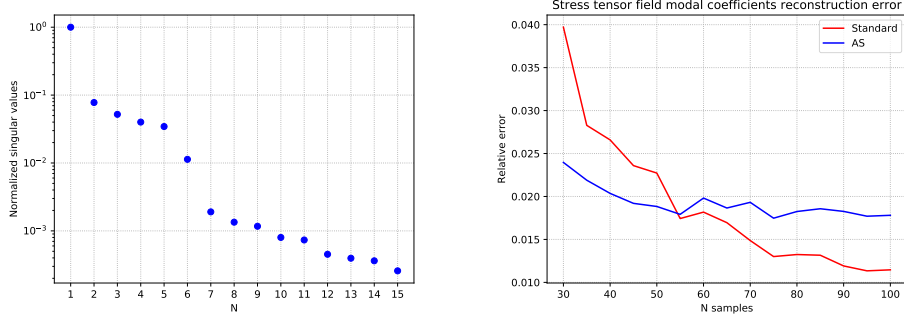


Figure 2: On the left the normalized singular values decay of the stress tensor field snapshots matrix. Only the first 15 are depicted, and we select only the first 6. On the right the relative error for the stress tensor field modal coefficients reconstruction using 5-fold cross validation for both the full parameter space and the active subspace (AS), as a function of the number of the samples.

4.2 Numerical study 2: pressure reconstruction in fluid dynamics with a parametric domain

We are now considering the flow around a square in a parametric domain, a standard benchmark in computational fluid dynamics. Since the used approach is completely data-driven, it is out of the purpose of this work the analysis of the mathematical model. We just provide an overview of the parametric formulation to give the opportunity to the reader to understand and replicate the results.

We have a rectangular domain in which an incompressible flow past a square cylinder. A sketch of the domain is depicted in Figure ???. The Γ_{in} , Γ_{out} and Γ_{wall} refer respectively to the inlet boundary, the outlet boundary and the physical wall of the domain. To stay in a steady regime, we impose a low Reynolds number ($Re = 13$). The incompressible Navier Stokes equations

$$\begin{cases} \frac{\partial u}{\partial t} + (u \cdot \nabla)u - \nabla \cdot \nu \nabla u = -\nabla p & \text{on } \Omega, \\ \nabla \cdot u = 0 & \text{on } \Omega, \end{cases} \quad (13)$$

are solved in the described domain using OpenFOAM [41], a open source library implementing finite volume (FV) method.

To parametrise and deform the original domain, we apply the free form deformation (FFD) technique [32] to the undeformed computational grid. It is a well-spread parameterisation method used to morph smoothly complex geometries. It consists on the composition of three maps:

1. a function ψ that transform the physical domain Ω to the reference

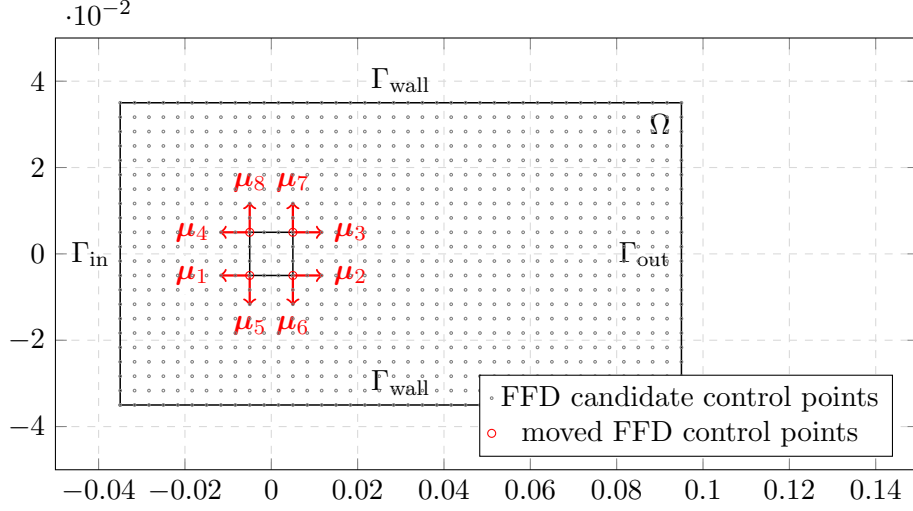


Figure 3: A sketch of the (undeformed) domain for the computational fluid dynamics simulation. The black dots are the FFD candidate control points, while in red we highlight the ones we move to morph the original domain.

domain $\widehat{\Omega}$;

2. the actual morphing done by the map T . It induces the transformation of $\widehat{\Omega}$ given the displacements of the FFD control points composing the lattice around the object to deform. It is based on tensor products of Bernstein polynomials. This produces $\widehat{\Omega}(\boldsymbol{\mu})$;
3. the back mapping from the reference domain to the physical one: $\psi^{-1} : \widehat{\Omega}(\boldsymbol{\mu}) \rightarrow \Omega(\boldsymbol{\mu})$.

The actual mapping takes the following form: $\mathcal{M}(\boldsymbol{\mu}) : \psi^{-1} \circ T \circ \psi(\boldsymbol{\mu})$.

In this work, we embedded all the domain into the FFD lattice of control points, moving only the 4 control points collocated on the internal square vertices. The number of parameters p is set to be equal to 8. This is the result of moving 4 FFD control points along the x - and y -directions (in Figure ?? the direction of the displacements is reported). The computational grid is deformed using the Python package PyGeM [1], implementing some of the most popular morphing technique as FFD, radial basis functions (RBF) interpolation, and inverse distance weighting (IDW). For more details about these methodologies, we suggest [4, 16, 28, 33, 2].

Once we collected all the numerical solutions for the 200 sampling configurations, we extract the pressure snapshots to compute the POD modes. Analyzing the singular values decay (Figure 4 on the left), we select the first 8 modes. After the projection of the samples onto the POD space, the active

subspace of dimension 1 is then computed for each modal coefficient. Figure 5 reports the AS accuracy by showing the approximation of the modal coefficients along the new active variable, that is $\alpha_i(\boldsymbol{\mu})$ against $\mathbf{W}_{1,i}^T \boldsymbol{\mu}$. As in the previous example, a radial basis function kernel has been chosen to perform the gaussian process regression to reconstruct the response surface in the active subspaces. We compare the accuracy of the data-driven model with the AS enhancement and using a standard approach: the latter refers to an interpolation in the full dimensional parametric space (\mathbb{R}^8) of the modal coefficients using a radial basis function. We compute the relative error with a CV technique, varying the number of snapshots used for the AS approximation and for POD modes computation (Figure 4 on the right). Using AS, the relative error is lower with respect to the standard approach with a limited set of high-fidelity snapshots and with only 20 samples the relative error is halved thanks to AS. Increasing the initial database dimension, the accuracy gain becomes less important and the standard interpolation provides better results, in this example using more than 55 initial samples, since the error introduced by AS approximation is greater than the interpolation error.

5 Conclusions and perspectives

In this work we presented a novel coupling between the active subspaces property and the non-intrusive reduced order method called proper orthogonal decomposition with interpolation. We proved the efficiency of the technique on two diverse benchmark problems involving geometrical parameterisation. The AS property is able to enhance the performance of PODI when the offline database of solutions is poor in terms of cardinality. This

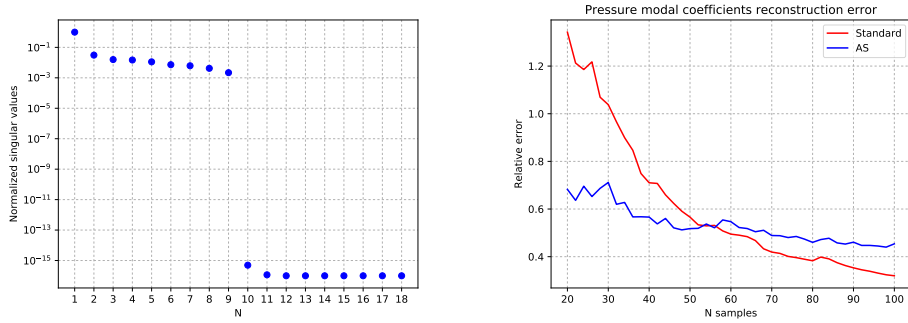


Figure 4: On the left the normalized singular values decay of the pressure snapshots. On the right the relative error for the pressure modal coefficients reconstruction using 5-fold cross validation for both the full parameter space and the active subspace (AS), as a function of the number of the samples.

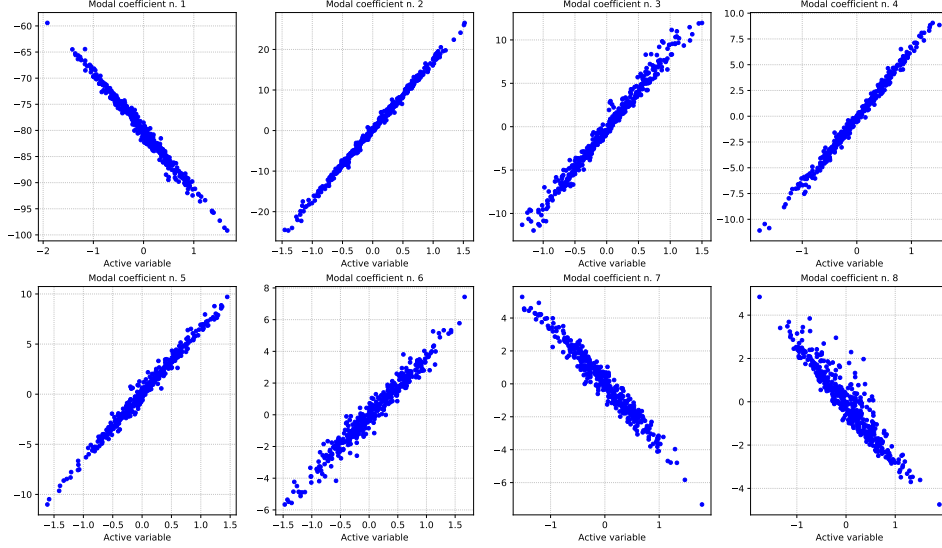


Figure 5: Sufficient summary plots for the pressure modal coefficients. The first 8 coefficients $\alpha_i(\boldsymbol{\mu})$ are represented along the corresponding active variable $\mathbf{W}_{1,i}^T \boldsymbol{\mu}$.

results in better reconstruction error of the output fields of interest for new untried input parameters. So the proposed method is useful especially when the offline phase of the reduced order model is computationally intensive. Nevertheless after a certain threshold, that means having enough samples of the full order solutions, the classical PODI over the full parameter space is more viable.

Future developments are required in order to have error bounds for the proposed method. Moreover, non linear extensions of the active subspaces property could be beneficial to improve the approximation accuracy.

Acknowledgements

This work was partially supported by an industrial Ph.D. grant sponsored by Fincantieri S.p.A., and by the European Union Funding for Research and Innovation — Horizon 2020 Program — in the framework of European Research Council Executive Agency: H2020 ERC CoG 2015 AROMA-CFD project 681447 “Advanced Reduced Order Methods with Applications in Computational Fluid Dynamics” P.I. Gianluigi Rozza.

References

- [1] PyGeM: Python Geometrical Morphing. Available at: <https://github.com/mathLab/PyGeM>.
- [2] F. Ballarin, A. D’Amario, S. Perotto, and G. Rozza. A POD-selective inverse distance weighting method for fast parametrized shape morphing. *International Journal for Numerical Methods in Engineering*, 117(8):860–884, 2019.
- [3] F. Ballarin, A. Manzoni, A. Quarteroni, and G. Rozza. Supremizer stabilization of POD–Galerkin approximation of parametrized steady incompressible Navier–Stokes equations. *International Journal for Numerical Methods in Engineering*, 102(5):1136–1161, 2015.
- [4] M. D. Buhmann. *Radial basis functions: theory and implementations*, volume 12. Cambridge university press, 2003.
- [5] T. Bui-Thanh, M. Damodaran, and K. Willcox. Proper orthogonal decomposition extensions for parametric applications in compressible aerodynamics. In *21st AIAA Applied Aerodynamics Conference*, page 4213, 2003.
- [6] T. Bui-Thanh, M. Damodaran, and K. E. Willcox. Aerodynamic data reconstruction and inverse design using proper orthogonal decomposition. *AIAA journal*, 42(8):1505–1516, 2004.
- [7] P. G. Constantine. *Active subspaces: Emerging ideas for dimension reduction in parameter studies*, volume 2. SIAM, 2015.
- [8] P. G. Constantine, E. Dow, and Q. Wang. Active subspace methods in theory and practice: applications to kriging surfaces. *SIAM Journal on Scientific Computing*, 36(4):A1500–A1524, 2014.
- [9] P. G. Constantine, M. Emory, J. Larsson, and G. Iaccarino. Exploiting active subspaces to quantify uncertainty in the numerical simulation of the hyshot ii scramjet. *Journal of Computational Physics*, 302:1–20, 2015.
- [10] M. Couplet, C. Basdevant, and P. Sagaut. Calibrated reduced-order POD–Galerkin system for fluid flow modelling. *Journal of Computational Physics*, 207(1):192–220, 2005.
- [11] N. Demo, M. Tezzele, G. Gustin, G. Lavini, and G. Rozza. Shape optimization by means of proper orthogonal decomposition and dynamic mode decomposition. In *Technology and Science for the Ships of the Future: Proceedings of NAV 2018: 19th International Conference on Ship & Maritime Research*, pages 212–219. IOS Press, 2018.

- [12] N. Demo, M. Tezzele, A. Mola, and G. Rozza. An efficient shape parametrisation by free-form deformation enhanced by active subspace for hull hydrodynamic ship design problems in open source environment. In *The 28th International Ocean and Polar Engineering Conference*, 2018.
- [13] N. Demo, M. Tezzele, A. Mola, and G. Rozza. A complete data-driven framework for the efficient solution of parametric shape design and optimisation in naval engineering problems. In *Proceedings of MARINE 2019: VIII International Conference on Computational Methods in Marine Engineering*, pages 111–121, 2019.
- [14] N. Demo, M. Tezzele, and G. Rozza. EZyRB: Easy Reduced Basis method. *The Journal of Open Source Software*, 3(24):661, 2018.
- [15] V. Dolci and R. Arina. Proper orthogonal decomposition as surrogate model for aerodynamic optimization. *International Journal of Aerospace Engineering*, 2016, 2016.
- [16] D. Forti and G. Rozza. Efficient geometrical parametrisation techniques of interfaces for reduced-order modelling: application to fluid–structure interaction coupling problems. *International Journal of Computational Fluid Dynamics*, 28(3-4):158–169, 2014.
- [17] F. Garotta, N. Demo, M. Tezzele, M. Carraturo, A. Reali, and G. Rozza. Reduced Order Isogeometric Analysis Approach for PDEs in Parametrized Domains. *Submitted, QUIET special volume*, 2018.
- [18] J. S. Hesthaven, G. Rozza, B. Stamm, et al. *Certified reduced basis methods for parametrized partial differential equations*. Springer, 2016.
- [19] E. N. Karatzas, G. Stabile, L. Nouveau, G. Scovazzi, and G. Rozza. A reduced basis approach for PDEs on parametrized geometries based on the shifted boundary finite element method and application to a Stokes flow. *Computer Methods in Applied Mechanics and Engineering*, 347:568–587, 2019.
- [20] R. Kohavi. A study of cross-validation and bootstrap for accuracy estimation and model selection. In *Proceedings of IJCAI-95*, volume 2, pages 1137–1145. Montreal, Quebec, 1995.
- [21] S. Lorenzi, A. Cammi, L. Luzzi, and G. Rozza. POD-Galerkin method for finite volume approximation of Navier–Stokes and RANS equations. *Computer Methods in Applied Mechanics and Engineering*, 311:151–179, 2016.

- [22] T. W. Lukaczyk, P. Constantine, F. Palacios, and J. J. Alonso. Active subspaces for shape optimization. In *10th AIAA multidisciplinary design optimization conference*, page 1171, 2014.
- [23] A. Mola, M. Tezzele, M. Gadalla, F. Valdenazzi, D. Grassi, R. Padovan, and G. Rozza. Efficient reduction in shape parameter space dimension for ship propeller blade design. In *Proceedings of MARINE 2019: VIII International Conference on Computational Methods in Marine Engineering*, pages 201–212, 2019.
- [24] A. Pinkus. Approximating by ridge functions. *Surface fitting and multiresolution methods*, pages 279–292, 1997.
- [25] A. Quarteroni, A. Manzoni, and F. Negri. *Reduced basis methods for partial differential equations: an introduction*, volume 92. Springer, 2015.
- [26] M. Ripepi, M. Verveld, N. Karcher, T. Franz, M. Abu-Zurayk, S. Görtz, and T. Kier. Reduced-order models for aerodynamic applications, loads and MDO. *CEAS Aeronautical Journal*, 9(1):171–193, 2018.
- [27] G. Rozza, M. W. Hess, G. Stabile, M. Tezzele, and F. Ballarin. Preliminaries and warming-up: Basic ideas and tools. In P. Benner, S. Grivet-Talocia, A. Quarteroni, G. Rozza, W. H. A. Schilders, and L. M. Silveira, editors, *Handbook on Model Order Reduction*, volume 1, chapter 1. De Gruyter, 2019.
- [28] G. Rozza, A. Koshakji, and A. Quarteroni. Free Form Deformation techniques applied to 3D shape optimization problems. *Communications in Applied and Industrial Mathematics*, 4(0):1–26, 2013.
- [29] G. Rozza, M. H. Malik, N. Demo, M. Tezzele, M. Girfoglio, G. Stabile, and A. Mola. Advances in Reduced Order Methods for Parametric Industrial Problems in Computational Fluid Dynamics. In R. Owen, R. de Borst, J. Reese, and P. Chris, editors, *ECCOMAS ECFD 7 - Proceedings of 6th European Conference on Computational Mechanics (ECCM 6) and 7th European Conference on Computational Fluid Dynamics (ECFD 7)*, pages 59–76, Glasgow, UK, 2018.
- [30] F. Salmoiraghi, F. Ballarin, G. Corsi, A. Mola, M. Tezzele, and G. Rozza. Advances in geometrical parametrization and reduced order models and methods for computational fluid dynamics problems in applied sciences and engineering: Overview and perspectives. *ECCOMAS Congress 2016 - Proceedings of the 7th European Congress on Computational Methods in Applied Sciences and Engineering*, 1:1013–1031, 2016.

- [31] F. Salmoiraghi, A. Scardigli, H. Telib, and G. Rozza. Free-form deformation, mesh morphing and reduced-order methods: enablers for efficient aerodynamic shape optimisation. *International Journal of Computational Fluid Dynamics*, 32(4-5):233–247, 2018.
- [32] T. Sederberg and S. Parry. Free-Form Deformation of solid geometric models. In *Proceedings of SIGGRAPH - Special Interest Group on GRAPHics and Interactive Techniques*, pages 151–159. SIGGRAPH, 1986.
- [33] D. Shepard. A two-dimensional interpolation function for irregularly-spaced data. In *Proceedings-1968 ACM National Conference*, pages 517–524. ACM, 1968.
- [34] G. Stabile, F. Ballarin, G. Zuccarino, and G. Rozza. A reduced order variational multiscale approach for turbulent flows. *Advances in Computational Mathematics*, pages 1–20, 2018.
- [35] G. Stabile and G. Rozza. Finite volume POD-Galerkin stabilised reduced order methods for the parametrised incompressible Navier–Stokes equations. *Computers & Fluids*, 173:273–284, 2018.
- [36] M. Tezzele, F. Ballarin, and G. Rozza. Combined parameter and model reduction of cardiovascular problems by means of active subspaces and POD-Galerkin methods. In D. Boffi, L. F. Pavarino, G. Rozza, S. Scacchi, and C. Vergara, editors, *Mathematical and Numerical Modeling of the Cardiovascular System and Applications*, pages 185–207. Springer International Publishing, 2018.
- [37] M. Tezzele, N. Demo, M. Gadalla, A. Mola, and G. Rozza. Model order reduction by means of active subspaces and dynamic mode decomposition for parametric hull shape design hydrodynamics. In *Technology and Science for the Ships of the Future: Proceedings of NAV 2018: 19th International Conference on Ship & Maritime Research*, pages 569–576. IOS Press, 2018.
- [38] M. Tezzele, N. Demo, A. Mola, and G. Rozza. An integrated data-driven computational pipeline with model order reduction for industrial and applied mathematics. *Submitted, Special Volume ECMI (W. Schilders ed.)*, 2018.
- [39] M. Tezzele, N. Demo, and G. Rozza. Shape optimization through proper orthogonal decomposition with interpolation and dynamic mode decomposition enhanced by active subspaces. In *Proceedings of MARINE 2019: VIII International Conference on Computational Methods in Marine Engineering*, pages 122–133, 2019.

- [40] M. Tezzele, F. Salmoiraghi, A. Mola, and G. Rozza. Dimension reduction in heterogeneous parametric spaces with application to naval engineering shape design problems. *Advanced Modeling and Simulation in Engineering Sciences*, 5(1):25, Sep 2018.
- [41] H. G. Weller, G. Tabor, H. Jasak, and C. Fureby. A tensorial approach to computational continuum mechanics using object-oriented techniques. *Computers in physics*, 12(6):620–631, 1998.